Analyzing Transient Cornering

Alex Stapleton, Peter Meyer, Bolun Zhang, Jonghyuk Oh

ABSTRACT

This paper investigated the transient characteristics of vehicle cornering.. In order to understand this process, a numerical model was built in Matlab based on the bicycle model introduced in class. The behavior of this vehicle model was studied in Matlab and observations were made regarding the effects on transient cornering due to changing relevant vehicle parameters. Also, a tire model was derived in an attempt to better understand transient effects on the tires themselves.

INTRODUCTION

During this semester, we studied the equations and qualitative behaviors that can be used to describe a vehicle subject to steady state cornering. However, a vehicle typically experiences transient cornering for a majority of its operating time. Furthermore, these transients determine how quickly or comfortably a vehicle enters into a turn. In other words, they are a key measure of vehicle handling and performance. Because of this, we attempted to create a model that described vehicle dynamics during this transient period by including some relevant variables.

Before jumping into the vehicle model, we looked into some qualitative descriptions of transient cornering found in literature **[1, 2]**. This research will allow for some insight into the best way to implement our model. Furthermore, it will provide a way for us to analyze the results of the vehicle model.

In class, when looking at steady-state cornering, we applied Newton's laws of motions with the assumption that yaw rate and roll angle are constant. During transient this is not the case. By removing these assumptions the analytical solutions to describe these transients were easy to obtain in differential form. However, they proved difficult to solve. As a result, numerical methods were applied to these equations and a model was developed. While our model proved to be limited in scope, we were able to use it to compare the effects of changing relevant vehicle parameters.

The change in the tires of the vehicle is also important when analyzing transient cornering. It is necessary to take into consideration the cornering and lateral stiffenesses of the tire in order to determine the deformation a tire undergoes when cornering. The contact patch acts as a spring when cornering and for simplification purposed, it will be assumed as a single point. The lateral and longitudinal deflection of the point will be analyzed.

Qualitative Description of Transient Cornering

To fully understand what is happening in transient cornering, it is important to make some assumptions and create a reference in which this transient event takes place. To begin, It is assumed that the car is moving straight ahead in steady state and at a given moment, the driver suddenly turns the steering wheel to a certain angle and holds the wheel there. This simulates a step input of the steering angle.

Turning Without Roll and No Understeer or Oversteer

At the very start of the turn, the driver turns the steering wheel at an angle, but the vehicle continues to go straight. Because of this, the front slip angle becomes equal to the front steer angle, which produces a lateral force only on the front of the vehicle. This causes rotational acceleration.

As the front end begins to move into the curve, the rear of the car follows, and a slip angle on the rear axle is created. This slip angle generates a lateral force on the rear tires. However, it does not produce a large effect, at first, due to the sizably larger lateral force on the front of the vehicle. After around ¾ of a second, the rear slip angle has increased and therefore the lateral force in the rear has also increased. The forces on the front and rear balance out the moment on the center of gravity and the car exits the transient stage. The time it takes to go through the transient process is not changed much when the steering angle or vehicle speed entering the curve is increased. However, he

distance travelled during the transition will increase.

The responsiveness of the car is characterized by two factors: 1) the length of the transition period and 2) the amount of instantaneous response. The lateral acceleration of the car are influenced by several factors such as the understeer and oversteer effects and cornering stiffness. If a vehicle has an understeer effect, then the car will reach equilibrium faster because it will reach the larger radius of curvature faster. An oversteer vehicle will reach equilibrium more slowly because it will have a smaller radius of curvature and therefore it will take longer to build up the lateral acceleration needed to turn. If you adjust the cornering stiffness, the rate of build-up of lateral acceleration will vary, but they will all reach the same equilibrium. A vehicle with high cornering stiffness will take less time to build up lateral acceleration because it will reach equilibrium faster at the instant the wheel is turned. A lower cornering stiffness is the opposite because it takes longer to reach the desired radius of curvature.

Turning when Accounting for Roll

When a lateral force is suddenly exerted on a vehicle, the center of gravity will lag behind the wheel movement. As the transient process begins, the roll angle will increase quickly during the first 0.2 seconds. The roll angle will then gradually increase until equilibrium is reached between the roll and curvature of the turn. If the vehicle has a higher roll center, the initial change in roll angle may not be as large during the first 0.2 seconds. However, the body roll angle may overshoot the equilibrium roll angle because the roll stiffness is much lower. Reducing the roll stiffness the correct amount is essential for optimal vehicle control.

The height of the roll center effects the lateral acceleration during the transient stage. An ideal situation would be a steady initial acceleration and a short transition time. Satisfactory vehicles also have the vehicle lateral acceleration and roll angle build up at the same rate. If they do not increase at the same rate, the roll angle may overshoot, creating a rough roll during cornering which causes rider discomfort.

Transient Cornering Equations and Model Development

In developing a model for transient cornering, we took an incremental approach. We first began with the bicycle model used to analyze steady state cornering. In doing so we made some basic assumptions to simplify our analysis. Then, we added into our model the effects of lateral load transfer from the inner to outer wheels.

To begin creating our model, we started with the bicycle model pictured in **Figure 1**. Using the relevant quantities shown in the figure and applying Newton's Laws, we were able to develop some simple equations which describe the dynamics of this model (1,2). In these equations, we introduced the assumption that the vehicle's forward velocity remains constant. In order to use these equations, some way of calculating slip angles is needed. Our method for calculating these, shown in equations 3 and 4, use the relationship between forward velocity and lateral velocity due to yaw velocity at each tire, with respect to the vehicle reference frame.

With these four equations, all that is needed to fully describe the transients of this bike model is tire cornering stiffness. When lateral load transfer is not being considered, it is a fair assumption to use a constant cornering stiffness that varies lateral tire forces linearly as slip angles change. However, since we wanted to include load transfer effects in our model, we decided to incorporate the lateral force carpet plots (**Figure 3**) used in class into our model. To do this, we created force versus slip angle curves fitted to data points for different normal force values. This is shown in **Figure 4.** The fitted equations were then used to interpolate lateral forces for a given slip angle and normal force.

To calculate the changing normal forces that occur due to lateral load transfer, we started by using the equations (6-9) from class describing steady-state vehicle roll. In order to incorporate them in the transient case, we included the roll angle acceleration and inertia terms. Also, it was necessary to add a damping term proportional to roll velocity into this equation that it resembles a real suspension during transients. Similar to the equations developed in class, we were able to calculate the difference between inside and outside normal forces by summing torques about the unsprung mass C.G (9).

The final part of creating this vehicle model was to apply appropriate length, height, and moment

parameters to the model. These parameters proved difficult to find in an all-inclusive form. Therefore, we used a few different sources for these. To calculate the moments of inertia for yaw and roll, we found an article by the NHTSA that provides empirical formulas for calculating these [source]. The heights and lengths of the C.G.s and roll center were determined based on values used in homework assignments.

EQUATIONS

Bicycle Model
θ: yaw angle
ϕ: roll angle
δ_f: steering angle
V: velocity
V_f: velocity of the front
V_r: velocity of the rear
r: yaw velocity
α_f: front slip angle
α_r: rear slip angle
$C_{\alpha f}$: front cornering stiffness
$C_{\alpha r}$: rear cornering stiffness
J_z: moment of inertia about z-axis
M: roll moment
a: distance from CG to the front wheel
b: distance from CG to the rear wheel
h_r: roll center height
h_u: unsprung mass height
F_{zi}: inside tire normal force
F_{zo}: outside tire normal force
F_{yi}: inside tire lateral force
F_{yo}: outside tire lateral force
F_{rc}: roll center force

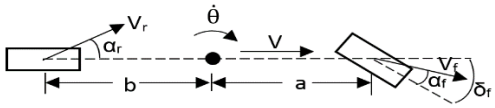

Figure 1. Bicycle Model

$$C_{\alpha r}\alpha_r + C_{\alpha f}\alpha_f cos(\delta_f) = M\ddot{y} \quad (1)$$

$$aC_{\alpha f}\alpha_f cos(\delta_f) - bC_{\alpha r}\alpha_r = Jz\ddot{\theta} \quad (2)$$

$$\alpha_r = tan^{-1}\left(\frac{b\ddot{\theta}}{V}\right) \quad (3)$$

$$\alpha_f = \delta_f - tan^{-1}\left(\frac{a\ddot{\theta}}{V}\right) \quad (4)$$

$$Jz = 0.9M\left(\frac{a+b}{2}\right)^2 \quad (5)$$

$$F_{rc} = M_s\ddot{y} \quad (6)$$

$$M - F_{rc}Rcos\phi - M_sgRsin\phi + c\dot{\phi} = J_s\ddot{\phi} \quad (7)$$

$$M = k_\phi\phi \quad (8)$$

$$(F_{zo} - F_{zi})\frac{t}{2} - h_c(F_{yi} + F_{yo}) - (h_r - h_u)F_{rc}$$

$$-M - c\dot{\phi} = 0 \quad (9)$$

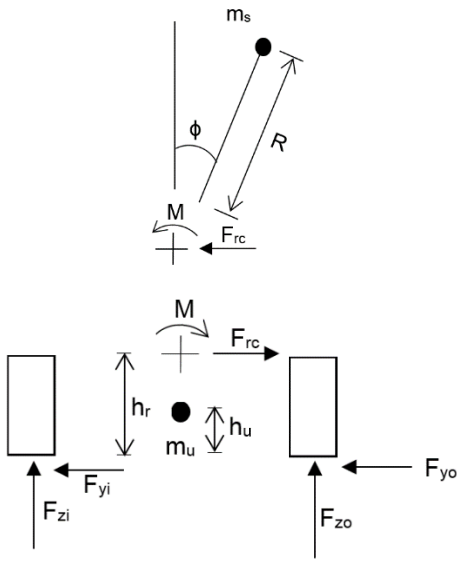

Figure 2.Lateral Load Transfer

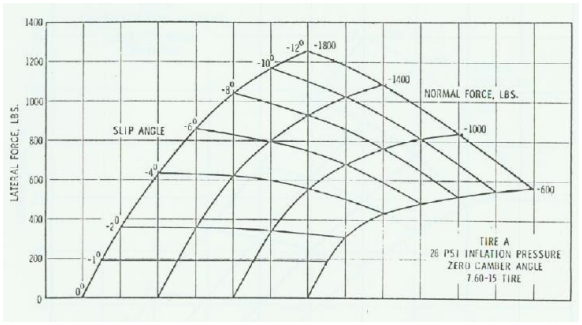

Figure 3. Lateral force carpet plots used to develop tire model.

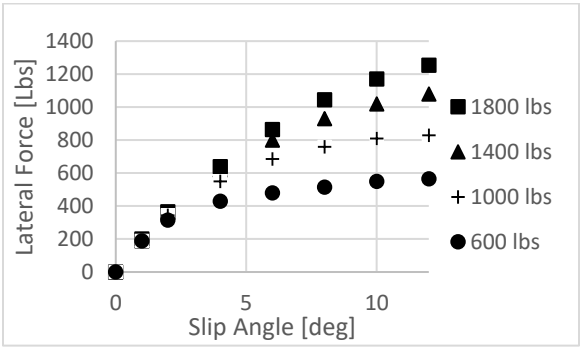

Figure 4. Lateral tire force lines for various normal force loads.

Analyzing Model Validity

The best way to determine whether or not this model accurately captures the dynamics during transient cornering is to compare yaw rate and

lateral acceleration results from our model to those found in published papers. The data found in these papers includes both measured data from actual vehicle tests as well as simulation results [**2-7**].

Figures 5-7 show some of the results obtained from our model for step inputs of steer angle at various speeds. These simulations were carried out with a "base model" of our vehicle. We define this model as one with even forward to rear weight distribution, equal cornering stiffness, and even distribution of roll stiffness. At first glance, these response profiles seem to match well with those seen in SAE literature. Response times for each variable is between 0.5 [s] and about 1 [s]. This fits both Shilling's qualitative description as well as actual response data given in research papers. Our responses, except for yaw rate, also show an overshoot before reaching steady state values. This dynamic behavior also agrees with the literature.

While our model seems to agree with some of the qualitative measures of transient response seen, a quantitative comparison shows that our model only has a narrow window of validity. In general, our model produces steady-state yaw velocities that are larger than those seen from other models. Conversely, our model produces steady-state lateral accelerations that our smaller than other models. One obvious explanation for this difference is that our vehicle parameters do not match those used in other models. However, this results remain fairly consistent when playing with model parameters.

Along those same lines, using information from literature to validate our model does have some drawbacks. First, the vehicle parameters used-such as wheelbase lengths, C.G. heights, vehicle weight, and tire stiffness-are rarely provided in a comprehensive and explicit way. Second, the results presented are usually only given for one set of speed and steer angle operating points. This makes it difficult to be confident in making comparisons to this data, and also limits our ability to validate how well our model predicts the effects of changing vehicle parameters on transient response.

The fact that our model lacks accuracy for larger velocities and steer angles doesn't come as a surprise in the end. There are a number of influences on transients coming from tires and suspension design which have not been included in our model. Examples of these influences include suspension dynamics, changing camber angles, roll steer, and tire dynamics. Due to our uncertainty in the accuracy of this model at higher speeds and steer angle, the remainder of our analysis will be for the case of 5 [deg] steer and 25 [m/s] velocity.

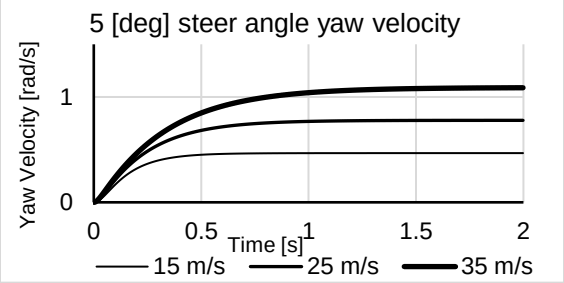

Figure 5. Yaw velocity response at various speeds for a steer angle of 5 [deg].

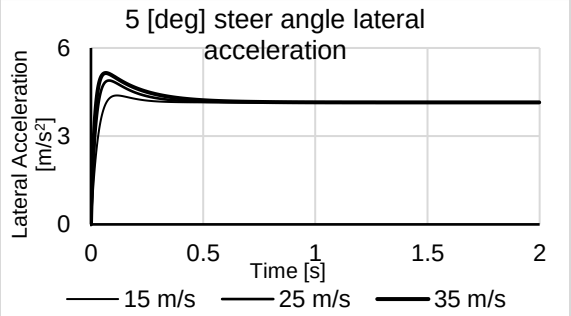

Figure 6. Lateral acceleration response at various speeds for a steer angle of 5 [deg].

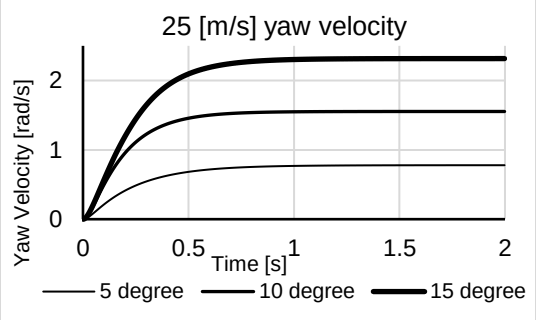

Figure 7. Yaw velocity response for various steer angles at 25 [m/s].

Effect of Vehicle Parameters on Transient Response

The first parameter we looked at was changing the distance from the front tire to the C.G. of the vehicle *a*. The effect this had on yaw velocity and lateral acceleration response are shown in **Figure 8** and **9.**

Looking at the transient responses, we can see that increasing *a* leads to an increase in response time for both yaw velocity and lateral acceleration. This could be viewed as having a negative effect on performance because the vehicle will take longer to respond to steering inputs. We can also see that the ratio of the steady-state yaw rate to lateral acceleration increases as *a* increases. This is indicative of an oversteer vehicle, which makes sense when we recall that the understeer coefficient will decrease as weight is shifted from the front to the rear of the vehicle.

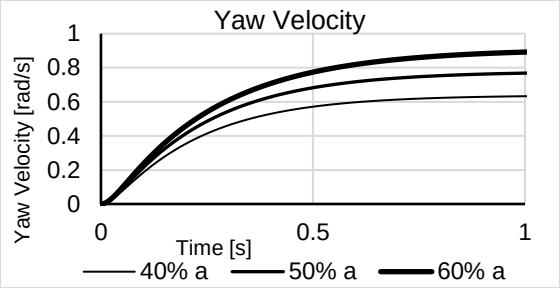

Figure 8. Yaw velocity response at 25 [m/s] and 5 [deg] step steer for various values of a as a percent of wheelbase.

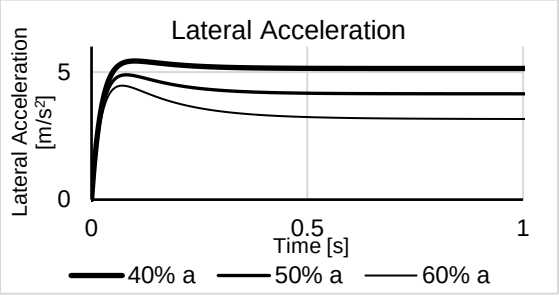

Figure 9. Lateral acceleration response at 25 [m/s] and 5 [deg] step steer for various values of a as a percent of wheelbase.

The second parameter we looked at was tire cornering stiffness. Specifically, we looked at how increasing cornering stiffness at the front or rear of the vehicle would affect transient response. Our results are shown in **Figure 10** and **11.** Our model shows that response time for yaw rate decreased in both cases when the front and rear stiffness were not equal. Also, increasing the front stiffness results in a greater yaw rate. This may seem favorable for improving cornering ability. However, looking again at understeer coefficient, doing this increases the oversteer characteristic which means decreasing stability at high speeds.

When we examine lateral acceleration, the total response time for the case of Cr = 2Cf is much faster than the others and also has no overshoot. This type of response would be most favorable for increasing performance. From what was found in literature, it seems that this is, in fact, the favored set up.

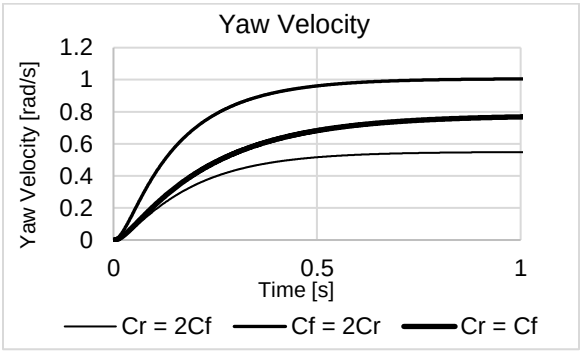

Figure 10. Yaw Velocity response at 25 [m/s] and 5 [deg] step steer for various ratios of front and rear tire stiffness.

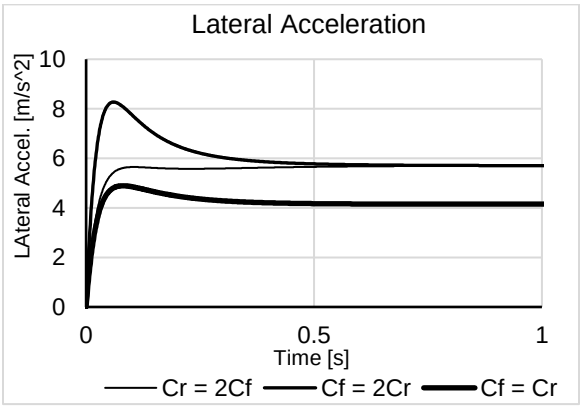

Figure 11. Lateral acceleration response at 25 [m/s] and 5 [deg] step steer for various ratios of front and rear tire stiffness.

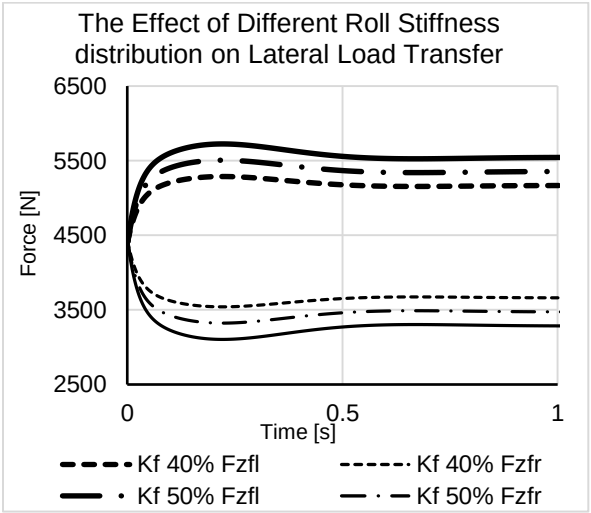

Figure 12. Lateral Load Transfer response of front tires at 25 [m/s] and 5 [deg] step steer for various roll stiffness of front and rear.

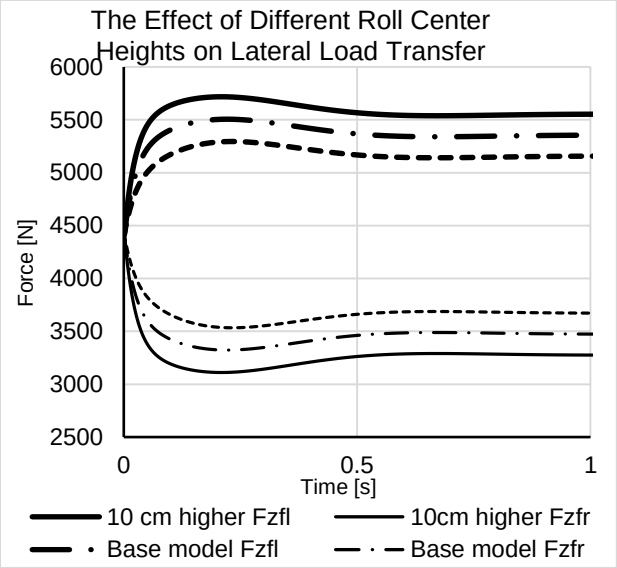

Figure 13. Lateral Load Transfer response of front tires at 25 [m/s] and 5 [deg] step steer for various roll center heights.

Another parameter we looked at was the front and rear roll stiffness distribution. It does not have significant effect on the yaw velocity and lateral acceleration because the steer angle is relatively small. Looking at our tire stiffness model, at low slip angles there is almost no difference in lateral force for different normal forces. Clearly, changing the roll stiffness distribution has a large effect on lateral load transfer, as shown in **Figure 12**. If the front roll stiffness is increased. This change enlarges lateral load transfer on the front tires, which leads to lateral force loss and contributes to understeer. The response times are about equal for different roll stiffness.

The effect of the roll center height was shown in **Figure 13**. Similar to roll stiffness, roll center height do not have large effect on lateral acceleration and yaw velocity, but it does on lateral load transfer. The higher roll center results in larger lateral load transfer, thus more lateral force loss and understeer.

Transient Tire Dynamics

The lateral force generated at the contact patch lags the generation of the tire slip angle (steer input). The reason for the lag is the relaxation effect of pneumatic tires and its deformation.

Relaxation Length

Relation length can be defined as the length that the tire has to travel in order for the lateral force that the tire is experiencing to reach 63.2% of the steady-state force after steer input. Equation 10 shows how lateral force can be calculated with lag included. Its effective relaxation length will be when the time (t) is equal time constant (T).

$$F_y = C_\alpha \alpha (1 - e^{-\frac{t}{\tau}}) \quad (10)$$

The relaxation length due to the sideslip angle is,

$$\sigma_\alpha = \frac{C_{F\alpha}}{C_{Fy}} \quad (10)$$

where $C_{F\alpha}$ is the cornering stiffness due to sideslip and C_{Fy} is the lateral tire stiffness [8,10]. There is also a relaxation length exhibited due to longitudinal forces. The equation is given by,

$$\sigma_\kappa = \frac{C_{F\kappa}}{C_{Fx}} \quad (11)$$

where $C_{F\kappa}$ is the cornering stiffness due to longitudinal slip ratio and C_{Fx} is the longitudinal tire stiffness [8,10]. Because only transient cornering is being analyzed in this paper, longitudinal relaxation length can is neglected.

Explanation of Single Point Contact Patch

When analyzing transient behavior of tires, there are many different methods used to describe how a tire reacts when not in steady-state. One the simplest theories, and recognized by many as a practical model, is the single point contact patch model. The contact patch, in reality, is the area of tire that is making contact with the ground and can vary depending on the mass of the vehicle, road conditions, or lateral tire stiffness. To observe transient behavior, it is easy to evaluate when assuming the contact patch is a single point. To see how a tire reacts to steering input, lateral and longitudinal deflection, *v* and *u* respectively, will be evaluated and equations will be derived to see how they change based on velocity and sideslip angle. The figure below displays the forces and velocities of the single point model.

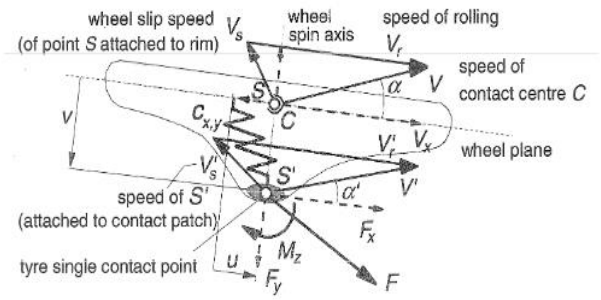

Figure 14: Single Point Contact Patch Model (Top View) [11]

Derivation of Equations

In Pacejka's book, *Tire and Vehicle Dynamics* [11], he breaks down the tire dynamics when in a transient state. When cornering, there will be a longitudinal and lateral force exerted on the contact patch. These forces cause the point to move in the x and y direction and act as a spring due to the elastic properties of the tire. The contact point will then have a slip velocity relative to the original tire velocity. The slip velocities are given by the following equations:

$$V_{sy} = |V\_x|\alpha \quad (12)$$

$$V_{sx} = (V_x - \omega r_e)/(V_x) \quad (13)$$

The lateral slip velocity, V_{sy}, is the x-direction velocity component multiplied by the sideslip angle because the angle will be small. The longitudinal slip velocity, V_{sx}, is the difference between the actual wheel velocity and the angular velocity of the wheel multiplied by the effective radius. These slip velocities are then used to find the change in deflection of the contact patch,

$$\frac{du}{dt} = -(V_{sx} - V'_{sx}) \ (14)$$

$$\frac{dv}{dt} = -(V_{sy} - V'_{sy}) \ (15)$$

When equations *14* and 15 are further converted they reveal the following differential equations for the lateral deflection due to sideslip and also lateral deflection due to camber angle,

$$\frac{dv_a}{dt} + \frac{1}{\sigma_a}|V_x|v_a = |V_x|\alpha = -V_{sy} \ (16)$$

$$\frac{dv_\gamma}{dt} + \frac{1}{\sigma_a}|V_x|v_\gamma = \frac{C_{F\gamma}}{C_{F\alpha}}|V_x|\gamma \ (17)$$

where $C_{f\gamma}$ is the camber stiffness for side force [9].

There is another differential equation involving the longitudinal deflection, *u*, however when cornering at a constant velocity, the change in longitudinal direction does not change much when compared to *v*, therefore it is omitted from this analysis. When solving these initial value differential equations the transient sideslip and camber angle values can be calculated.

$$\alpha' \approx \frac{v_\alpha}{\sigma_\alpha} \ (18)$$

$$\gamma' = \frac{C_{F\alpha}v_\gamma}{C_{F\gamma}\sigma_\alpha} \ (19)$$

Results

Solving the above differential equations using EES functions shows how the lateral deflection due to sideslip changes as the slip angle is incrementally changed. The below graph describes a turning even where the sideslip angle is increased to 1°.

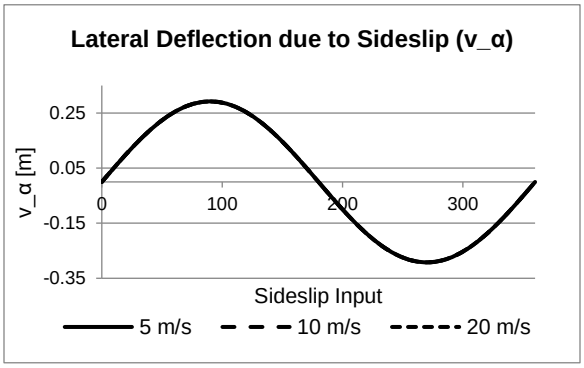

Figure 15: Lateral deflection due to slip angle with changing velocity

As shown on the above graph, all three velocity plots lie on the same line. There is a slight variation between the three velocities plots with an average difference of about 0.04 mm per degree of slip angle, proving the difference is minimal. This graph shows that with changing velocity minimally changes the lateral deflection due to sideslip.

When the sideslip angle is increased, there are more noticeable changes.

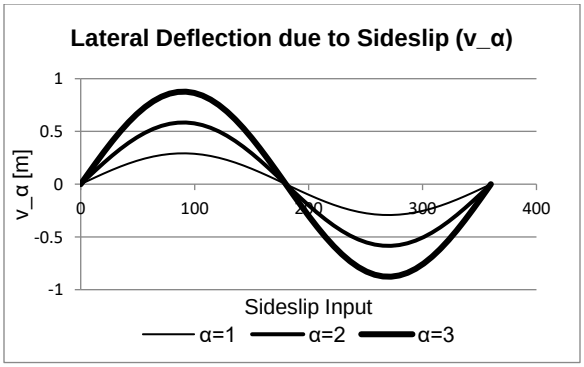

Figure 16: Lateral deflection due to sideslip with changing slip angle input

As seen when the sideslip angle is varied, the lateral deflection increases linearly with sideslip angle. The greater the steer angle input means a larger sideslip angle exhibited. This will, in turn, increase the lateral distance that the contact patch point with move relative to steady state.

When assessing the change in lateral deflection due to camber angle, the velocity variable was modified to visualize the changes. As seen with the sideslip angle, the lateral deflection due to camber angle also does not change significantly with increased velocity.

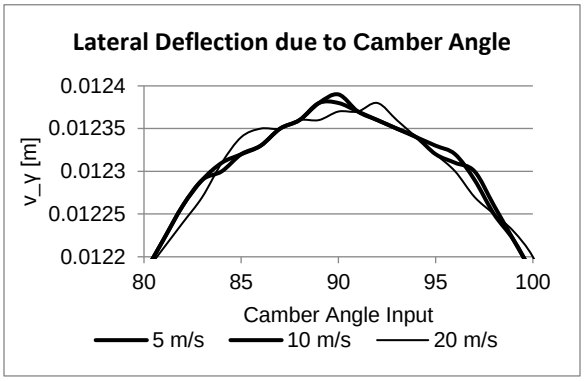

Figure 17: Lateral deflection due to camber angle with changing velocity

The above graph shows that the deflection changes, on average, the same no matter the velocity input. Changing the camber angle input also conducted and simulated. The results were similar to sideslip input change in that the lateral deflection increased as camber angle increased.

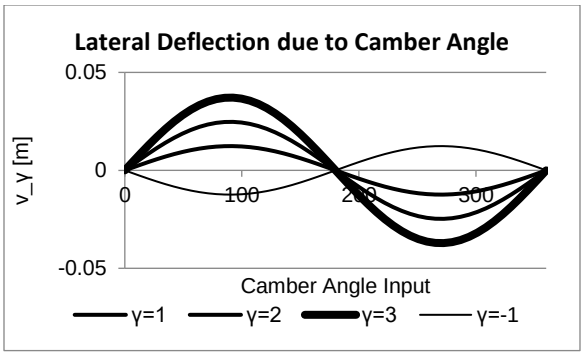

Figure 18: Lateral deflection due to camber with changing camber angle input

When comparing the two graphs involving changing the sideslip and camber input, it can be seen that the lateral deflection due to sideslip is much greater (almost 30 times more) than the lateral deflection due to camber angle. This is because the sideslip causes a greater lateral force than camber due to the tire stiffnesses ($C_{F\alpha} > C_{F\gamma}$).

Conclusion

In analyzing transient cornering, there are a number of different factors that need to be considered in order to achieve an accurate model. However, using a simple bicycle model, we were able to create a model that described some of the qualitative features of transient cornering well. Using this, we were able to analyze how changing vehicle parameters can affect a vehicle's response and performance characteristics associated with this.

Analyzing tires when in transient cornering shows that the contact patch will move like a spring based on lateral and longitudinal forces. Based on the model that was created, it was determined that the longitudinal distance will not change when the vehicle is cornering. If the velocity of the vehicle is increased when entering a turn, the lateral deflection of the contact patch will minimally change. Changing the slip angle or camber angle will change the deflection linearly. For tire deformation, the lateral deflection due to sideslip angle is a far greater influence on the total deflection than the deflection due to camber angle.

1. Milliken, W.F. and Milliken, D.L., “Chassis Design Principles and Analysis,” SAE International, Warrendale, PA, ISBN 978-0-7680-0826-5, 2002.
2. Wu, X. Farhad, M. Wong, J., “Investigating and Improving Vehicle Transient Handling Performance,” SAE Technical Paper 2011-01-0987, 2011, doi:10.4271/2011-01-0987.
3. Barak, P. Tianbing, S., “On Body Roll Angle During Transient Response Maneuver of a 3-D Model,” SAE Technical Paper 2003-01-0963, 2003, doi:10.4271/2003-01-0963.
4. Kodaira, T. Ooki, M. Sakai, H., “Vehicle Transient Response Based on Human Sensitivity,”SAE Technical Paper 2008-01-0597, 2008, doi: 10.4271/2008-01-0597.
5. Chee, W. “Measuring Yaw Rate with Accelerometers,” SAE Technical Paper 2001-01-2535, 2001, doi: 10.4271/2001-01-2535.
6. Hopkins, B. Taheri, S. Ahmadian, M., “Yaw Stability Control and Emergency Roll Control for Vehicle Rollover Mitigation” SAE Technical Paper 2010-01-0901, 2010, doi:10.4271/2010-01-1901
7. Ghosh, S. Deb, A. Mahala, M. Tanbakuchi, M. Makowski, M., “Active Yaw Control of a Vehicle using a Fuzzy Logic Algorithm,” SAE Technical Paper 2012-01-0229, 2012, doi:10.4271/2012-01-0229
8. Miller, S., et. al., “Calculating Longitudinal Wheel Slip and Tire Parameters Using GPS Velocity,” Proceedings of the AACC 0-7803-6459-3, 2001.
9. Dixon, J.C. (1996). Tires, Suspension and Handling 2nd ed. Warrendale: Society of Automotive Engineers.
10. Schmid, Markus, “Tire Modeling for Multibody Dynamic Applications,” Technical Report 2011-02, August 2011.
11. Pacejka, Hans, “Tire and Vehicle Dynamics,” SAE International, Warrendale, PA, ISBN 0-7680-1702-5, 2006